

Cite this: *Mater. Adv.*, 2025,  
6, 9817

# Test-tube model for rapid and accelerated biodegradation of poly(lactic acid)/poly(butylene succinate) blended bioplastic obtained from solution casting

Shreetam Parida,<sup>a</sup> Nivethitha Ashok<sup>a</sup> and Rajendra Kurapati<sup>id</sup> \*<sup>ab</sup>

Developing an alternative accelerated biodegradation test to the standard tests is crucial for the swift assessment of bioplastics to reduce the time duration and cost. Designing a blended bioplastic with an acceptable extent of miscibility in the polymeric phase and its rapid and accelerated real-time degradation is a persistent challenge because of its different chemical and crystalline properties. Hereby, we developed miscible blended bioplastic films of biopolymers poly(lactic acid) (PLA) and poly(butylene succinate) (PBS) with varied ratios by a simple solution casting method. The as prepared bioplastic blends of PLA/PBS (50/50 and 20/80) showed high miscibility with fascinating morphology as confirmed by optical and electron microscopy. Furthermore, the PLA/PBS films were validated by physicochemical methods including infrared spectroscopy, powder X-ray diffraction, thermogravimetric analyses and wettability by the contact angle measurements. All the results confirmed the successful preparation of blended bioplastics of PLA/PBS. Next, we developed a test-tube model for rapid and accelerated biodegradation (RAB) of the developed bioplastic blends of PLA/PBS in the form of films and powder (microparticles) using mobilised enzymes such as proteinase K and lipase in the aqueous buffer. The extent of degradation of the blends was followed using the physicochemical methods, along with the weight loss measurements. All the RAB results suggested that changes in surface area (from films to microparticle powder) affected the extent of enzymatic degradation of the bioplastic films and powder.

Received 29th June 2025,  
Accepted 26th October 2025

DOI: 10.1039/d5ma00690b

rsc.li/materials-advances

## 1. Introduction

Excessive plastic use and the gathering of waste have had a severely negative effect on environmental and ecological factors.<sup>1</sup> Plastic packaging materials made from synthetic polymers are mostly single-use and generally discarded once they are used. In total, 40% of petrochemical-based plastics are being used for packaging purposes and nearly 60% of plastic packaging products are used to pack food and beverages.<sup>1</sup> About 95% of plastic packaging products are wasted after a single use and end up in landfills, where they disintegrate into micro- or nanoplastics.<sup>1</sup> It has also been found that microplastics and their particles are found in milk, meat, and other edible items and have a direct impact on human health.<sup>2,3</sup> One of the solutions to reduce the environmental risk of

non-degradable plastic is by using alternative biodegradable bioplastics made from renewable materials (*e.g.*, biomass from corn and sugarcane), which undergo biodegradation by the action of microorganisms found in the soil.<sup>4</sup> However, biodegradable plastics have replaced conventional plastics to a very limited extent. Biodegradable polymers such as poly(lactic acid) (PLA), poly(glycolic acid) (PGA), poly(caprolactone) (PCL), poly(butylene adipate-*co*-terephthalate) (PBAT), and poly(butylene succinate) (PBS) have been used exclusively for manufacturing biodegradable plastics.<sup>5</sup> Furthermore, the European Bioplastics Organization forecasted that PLA and PBS would be the most demanded polymers for bioplastic applications by 2026, due to their applications in the biomedical and pharmaceutical industries.<sup>6,7</sup> In general, biopolymers are known to have lower mechanical strength compared to synthetic polymers.<sup>8</sup> For example, the usage of PLA in biomedical applications and packaging is limited because of its high brittleness.<sup>9</sup> Therefore, blending PLA with other biopolymers such as PBS could enhance the flexibility and processability while maintaining the biodegradability. Being a biodegradable polyester, PBS has high processing ability, thereby PLA/PBS blended bioplastics are used in various

<sup>a</sup> School of Chemistry, Indian Institute of Science Education and Research Thiruvananthapuram, Maruthamala P.O., Vithura, Thiruvananthapuram, Kerala 695551, India. E-mail: rkurapati@iisertvm.ac.in

<sup>b</sup> The Centre for Advanced Materials Research with International Engagement (CAMRIE), Indian Institute of Science Education and Research Thiruvananthapuram, Maruthamala P.O., Vithura, Thiruvananthapuram, Kerala 695551, India



applications. However, making blends of PLA/PBS is limited by incompatibility due to the lower chain entanglement across the interface. To improve the compatibility and flexibility of bioplastic blends, third components such as other biopolymer materials (e.g., bamboo powder, wood flour and cellulose fibres) were used to obtain the PLA/PBS blends.<sup>9</sup> Blend miscibility or compatibility persisted as a challenge, which is the key requirement for packaging, biomedical and biodegradation purposes.<sup>10–13</sup> Therefore, developing a PLA/PBS blend with good miscibility is a challenge without adding a third biopolymer, as mentioned. PLA/PBS blends have been achieved by using thermo-mechanical methods such as melt-extrusion, batch mixing by screw extrusion, compression moulding, *etc.*<sup>14,15</sup>

On the other hand, though various biodegradable plastics are emerging as alternatives to conventional non-biodegradable plastics, testing for the biodegradation of such biodegradable plastic materials involves a variety of standard tests with many parameters, thereby requiring a longer time, and is expensive.<sup>10</sup> The various standard tests for checking biodegradability are conducted under specified conditions, including realistic parameters and varied periods from 14 days to 24 months.<sup>16</sup> Furthermore, the International Standard Organisation (ISO) recommends many standard tests for assessing the biodegradability of biodegradable plastics, including in soil, seawater, marine sediment, *etc.*, which are regularly updated.<sup>17</sup> Also, the European Union (EU) recommended a series of standard biodegradation methods or tests. According to the European Chemical Agency (ECHA) report, there are three generalized categories of aerobic biodegradation, namely inherently degradable (minimum degradation is 70% within 14 days), readily degradable (minimum degradation is 60% within 28 days) and ultimately degradable (minimum degradation is 90% within 6 months for aqueous, 24 months for soil or seawater/sediment).<sup>16,18</sup>

However, assessing the biodegradability of biodegradable plastics following standard methods is a big hurdle as it takes a long duration (months to years) following various realistic conditions (soil, seawater, *etc.*), which will result in an increase in the cost of newly developed biodegradable plastics.<sup>19</sup> Therefore, alternative methods such as accelerated biodegradation tests have been developed to obtain rapid biodegradability of the biodegradable bioplastics. The accelerated tests involve treating the bioplastic directly with isolated microbial enzymes (from soil or seawater, *etc.*), varied size of the bioplastic particles (to increase the surface area), incubation at higher temperatures, and varied pH (to improve the enzymatic catalysis), organic solvents, pre-treatments, adding enzyme modifiers, *etc.*<sup>19–23</sup> Development of such rapid and accelerated biodegradation (RAB) tests is crucial for assessing the biodegradability of newly developed biodegradable bioplastics in a rapid manner. However, rapid biodegradation under accelerated conditions is still challenging to design. Such accelerated degradation methods could help to make a faster assessment of the degradation behaviour of newly developed bioplastics or biodegradable plastics.

PLA/PBS is a commonly used bioplastic blend for biomedical and packaging applications, but the biodegradability of PLA/PBS blended bioplastics is poorly understood. Therefore, the biodegradation of PLA/PBS blends needs to be understood thoroughly. Hence, designing a test tube model of “rapid and accelerated biodegradation (RAB)” for studying the degradation of bioplastics (PLA/PBS blends) using accelerated conditions, varying particle size, higher temperature, and enzyme modifiers would be interesting in this regard.

Unlike physical or chemical methods, enzymatic degradation leverages the natural capabilities of microbial enzymes to break down plastics efficiently. Microbial enzymes, capable of using plastics as their sole carbon source, have shown significant potential in accelerating the degradation process compared to traditional methods. Degradation of plastics by microbial enzymes offers a strategy to depolymerise waste petro-plastics into monomers for recycling or to mineralise them into carbon dioxide (CO<sub>2</sub>), water (H<sub>2</sub>O), and new biomass while producing higher-value bioproducts.<sup>21,24,25</sup> Herein, we developed the bioplastic of PLA/PBS using a simple solution casting method (varying the composition of PLA and PBS, PLA/PBS-80/20, 50/50, 20/80) with acceptable miscibility and the plastic was characterised using spectroscopic and thermal gravimetric techniques. Next, the obtained bioplastic was subjected to rapid accelerated biodegradation (RAB) by varying particle size, at higher temperature *via* enzymatic hydrolysis by proteinase K from *Tritirachium album*, lipase acrylic resin, and lipase from *Pseudomonas* sp.

## 2. Materials and methods

### 2.1. Materials

Poly(lactic acid) of PLAX175 grade was purchased from Banka Biolo Ltd, Hyderabad, India, with a molecular weight of 88 943 g per mole obtained from gel permeation chromatography (GPC). BioPBS<sup>TM</sup> (FZ79AC) grade poly(butylene succinate) was purchased from Tanhim Enterprise Pvt. Ltd, Greater Noida West, India, possessing a density of 1.26 g cm<sup>-3</sup>, and a molecular weight of 65 840 g per mole obtained from GPC. Chloroform was purchased from Merck Millipore. Dimethyl formamide (DMF, HPLC grade, assay > 99.9%) and KBr (>99.9% assay) were purchased from Sigma Aldrich. DSC alumina crucibles (Tzero pans) were purchased from TA Instruments, USA. Proteinase K (600 mAnson-U per mL; lyophilized powder, molecular biology grade) enzyme derived from *Tritirachium album*, lipase acrylic resin expressed in *Aspergillus niger*, and lipase from *Pseudomonas* sp. (type XIII, lyophilized powder) were all purchased from Sigma Aldrich. Co., USA.

### 2.2. PLA and PLA/PBS blended bioplastic film preparation

Pristine PLA and a blend of PLA/PBS (80/20, 50/50, 20/80) were taken at 4, 5, 8, 10, and 15 wt% and dissolved in chloroform under continuous stirring for either 2 h or 4 h at 65 °C to obtain miscible solutions.<sup>13,26</sup> Next, those miscible solutions were immediately cast on Petri-dishes (diameter 14.5 cm). Following solvent



evaporation, the sample was incubated slowly in an incubator overnight at room temperature. The obtained PLA/PBS films were slowly delaminated from the Petri plates from the corner (to avoid cracking and stretching) and dried in an oven at 65 °C for 48 h to remove extra solvent retained in the film matrix. It was observed that, except for the 4 wt% solution, the other weight percentage solutions resulted in hard, uneven and brittle blends. However, the 4 wt% solution under continuous stirring for 4 h at 65 °C formed very flat and smooth films, including for the pristine PLA and blends of PLA/PBS of 80/20, 50/50 and 20/80, as shown in Fig. S1.

### 2.3. Preparation of PLA and blended bioplastics of PLA/PBS powder

Cryogenic grinding was applied to obtain the powder form of the bioplastic blends using liquid nitrogen. Briefly, the prepared PLA film and PLA/PBS blended films were kept under cryogenic conditions by dipping in liquid nitrogen, and the films were immediately subjected to grinding using a BOSCH® mixer (Bosch TrueMixx Radiance Mixer Grinder 600 Watt, MGM4334RIN, Red) until all the films turned into a powder. Liquid nitrogen makes the PLA, PBS and PLA/PBS blends glassy or brittle, thereby helping in the powder formation. The prepared powders were segregated or separated using stainless steel sieves (sieve size range: Indian standard 469/1972, A.S.T.M. mesh number: 60 and 35 with coarse sizes 200 micron and 500 micron, respectively) to obtain microparticles in the range of 200–350 µm and 500–700 µm.

### 2.4. Rapid and accelerated biodegradation (RAB) of PLA and blended PLA/PBS bioplastic

**2.4.1. Biodegradation of the PLA film and PLA/PBS blended films by proteinase K.** PLA films and PLA/PBS blended films (80/20, 50/50, 20/80) of dimensions 7 × 7 mm<sup>2</sup> with thickness 4.1 ± 0.1 µm (film volume ~0.196 mm<sup>3</sup>) were incubated with mobilised proteinase K (from *Tritirachium album*) under RAB conditions, including shaking at 110 ± 5 rpm in 0.1 M Tris–HCl at a pH of 8.1 and temperature of 49 ± 1 °C.<sup>27,28</sup> The film to enzyme ratio was maintained (1 mg µL<sup>-1</sup>). First, 15 mg of pristine polymeric film or blended films was taken in a 1 mL vial containing 15 µL of proteinase K enzyme (with activity 600 mAnson) dissolved in 1.5 mL of 0.1 M Tris–HCl buffer solution, incubated at 49 ± 1 °C at 110 ± 10 rpm for 12 h, 3 days, and 7 days. The enzyme mixed buffer solutions were changed every 48 h to retrieve the original activity of the enzyme in the system.<sup>29</sup> The pristine and blended films were taken in 4 separate vials per each film labelled as control (buffer and film without enzyme) alongside 12 h, 3 days and 7 days samples (enzyme buffer solution and film) as shown in Fig. 4b. The aliquots were collected after every 12 h, 3 and 7 days of RAB incubation and immediately washed with an ethanol/water mixture at least three times to remove denatured enzymes and buffer. Next, the washed samples were dried at 65 °C for 48 h and stored under vacuum for the physicochemical characterisation to estimate the degradation percentage and structural changes.

**2.4.2. Biodegradation of the PLA film and PLA/PBS blend powders by proteinase K.** Microparticles with two different sizes, 200–350 µm and 500–700 µm, of the pristine PLA and PLA/PBS blends were obtained from cryogenic grinding as mentioned above. Similar to the bioplastic films, the bioplastic microparticles were also incubated using mobilised proteinase K (from *Tritirachium album*) under RAB conditions. Similar to the films, 15 mg of pristine polymeric powder or blended powder was taken in a 1 mL vial containing 15 µL of proteinase K enzyme (*i.e.* 1 mg of polymer per 15 µL of enzyme with activity 600 mAnson) dissolved in 1.5 mL of 0.1 M Tris–HCl buffer solution, incubated at 49 ± 1 °C at 110 ± 10 rpm for 12 h, 3 days, and 7 days. The enzyme mixed buffer solutions were changed every 48 h to retrieve the original activity of the enzyme in the system.<sup>29</sup> The pristine and blended powders were taken in 4 separate vials per each film labelled as control (buffer and film without enzyme) alongside 12 h, 3 days and 7 days samples (enzyme buffer solution and film) as shown in Fig. 4c. The samples were collected after 12 h, 3 and 7 days of RAB incubation, followed by washing with an ethanol/water mixture at least 3 times to remove denatured enzymes and buffer. Next, those collected samples were dried at 65 °C for 48 h and stored under vacuum for characterisation to estimate the degradation percentage and structural changes.

**2.4.3. Biodegradation of the PLA film using immobilised lipase.** Next, the biodegradation of the pristine PLA film was also carried out under the above-mentioned RAB conditions using an immobilised enzyme with 5 mg/0.27 cm<sup>3</sup> (enzyme to film volume) in a non-aqueous medium of toluene, *i.e.* lipase acrylic resin expressed in *Aspergillus niger*, to estimate the impact of organic solvent and immobilised enzyme on degrading the bioplastic PLA films.<sup>30</sup>

**2.4.4. Biodegradation of the PBS bioplastic film and PLA/PBS blended films using lipase.** RAB of the pristine PBS films and PBS in PLA/PBS (80/20, 50/50, 20/80) blended bioplastic films (dimensions 3 × 3 × 0.004 mm<sup>3</sup>) was also carried out under the aforementioned RAB conditions using lipase (from *Pseudomonas* sp. 1 mg mL<sup>-1</sup> film to enzyme buffer solution ratio quantity per film) in 0.5 mL of 0.1 M phosphate buffer at pH 7.2. Next, the resulting samples were characterised to estimate the degradation percentage.<sup>31–33</sup>

### 2.5. General characterisation methods

The thickness of the pristine and PLA/PBS blended bioplastics was measured using a KLA Tencor, D-600 model profilometer under room temperature conditions, maintaining a 2 mg stylus force and a 2.5 µm surface range with a 0.05 mm s<sup>-1</sup> speed. Fourier transform infra-red spectroscopy (FTIR) analyses of the obtained bioplastic films of PLA, PBS, blended PLA/PBS (80/20, 50/50 and 20/80) and powder samples were analysed using the IR grade KBr pellet method in an IR Prestige-21 Fourier Transform Infrared spectrophotometer, Shimadzu, Japan. Samples were analysed until 50 scans under a frequency range of 400–4000 cm<sup>-1</sup>. Similarly, degraded pristine PLA, pristine PBS, and PLA/PBS blends were also analysed.

Next, scanning electron microscope (SEM) analysis of the bioplastic films and powders was performed by mounting the



samples (films and powders) on carbon tape placed on aluminium stubs, which hold the films or powders properly for sputtering and analysis. The samples were made conductive with gold sputtering before imaging in a Nova NanoSEM 450 (NPE206 EDS/WDS) instrument, maintaining 15 kV to observe the clear surface images of the films and powders. Degraded pristine PLA, pristine PBS, and PLA/PBS blends were also characterised to get a clear view of the degraded samples according to the real-time frames.

The films and powders were subjected to X-ray irradiation in the specimen holder in a PanAnalytical PXRD (wide angle) system with a Cu K $\alpha$  source ( $\lambda = 1.5405 \text{ \AA}$ , 45 kV, 30 mA). The  $2\theta$  angles were set in the range of  $5^\circ$ – $60^\circ$ , provided with a  $1^\circ$  per minute scan rate at room temperature conditions for all the samples. Degraded pristine PLA, pristine PBS, and PLA/PBS blends were also diffracted under the same conditions to understand the structural changes.

Thermogravimetry analysis (TGA) of the PLA, PBS, PLA/PBS (80/20), PLA/PBS (50/50), and PLA/PBS (20/80) bioplastic films was carried out using the STA200 Thermal Analysis System (HITACHI Japan). All the samples were placed in an alumina crucible by taking 1–2 mg of each of the samples and the temperature was set from  $28^\circ$ – $600^\circ \text{ C}$  at a rate of  $10^\circ \text{ C min}^{-1}$  under inert conditions maintained by  $\text{N}_2$  gas as the supply gas ( $100 \text{ ml min}^{-1}$ ) and protecting gas ( $100 \text{ ml min}^{-1}$ ) to observe the TGA degradation curves and phase miscibility and composition.

Differential scanning calorimetry (DSC) was also carried out using the DSC Q20 (TA Instruments, USA) system for all samples to understand the phase miscibility and crystallinity of the blended films. A nitrogen atmosphere was maintained throughout the experiments. Samples were ramped from  $40$ – $200^\circ \text{ C}$  with a  $20^\circ \text{ C min}^{-1}$  rate and cooled down with the same rate to avoid any errors or moisture in the sample. Then the ramp was set from  $5$ – $200^\circ \text{ C}$  with a  $10^\circ \text{ C min}^{-1}$  rate to produce the data. The glass transition temperatures ( $T_g$ ), cold crystalline temperatures ( $T_{cc}$ ), and melting temperatures ( $T_m$ ) were observed for all the samples.

Polymer concentrations were maintained at  $8 \text{ mg mL}^{-1}$  in dimethyl formamide (DMF) purchased from Sigma Aldrich (HPLC grade, assay  $> 99.9\%$ ) and stirred until they dissolved completely. The solution was later filtered using a Merck filter (porosity  $0.45 \mu\text{m}$ ) before being taken for sample injection in the Infinity GPC/SEC system from Agilent Technologies, US, with a flow rate of solvent (DMF was stabilised with  $0.1\% \text{ LiCl}$ ) of  $0.5 \text{ mL min}^{-1}$  and a purge run of 600 s. Columns were heated at  $50^\circ \text{ C}$  to run all of the undegraded PLA, PBS and degraded PLA and PBS samples. Number average molecular weight ( $M_n$ ), weight average molecular weight ( $M_w$ ), and polydispersity index PD were obtained for the injected samples.

The water contact angle (WCA) of the undegraded and degraded PLA, PBS, PLA/PBS (80/20), PLA/PBS (50/50), and PLA/PBS (20/80) films were observed using the sessile drop method in the Drop Shape Analyser KRUSS instrument, Germany, with the gravitational acceleration of  $9.80665 \text{ m s}^{-2}$ . WCA for all

the samples was observed in the range of  $70$ – $100^\circ \text{ C}$ . Degraded pristine PLA, pristine PBS, and PLA/PBS blends were also observed to understand the changes in the nature of the film surfaces after hydrolysis.

**2.5.1. Estimation of physical weight loss.** Weight loss calculations were carried out after the proper drying of the collected degraded bioplastics at different time intervals. The microgram weights of the samples before degradation ( $W_{ud}$ ) and after degradation ( $W_d$ ) were taken using a Mettler Toledo weighing balance. The below-mentioned reported formula was used to calculate the percentage of matrix weight loss of each and every film/blend after every 12 h, 3 days, and 7 days of study to have a real-time calculation.<sup>34</sup>

$$\text{Weight loss (\%)} = \frac{(W_{ud} - W_d) \times 100}{W_{ud}}$$

## 2.6. Results and discussion

**2.6.1. Preparation of PLA/PBS miscible blends.** Fabrication of the PLA/PBS blend bioplastic is essentially achieved using the melt extruder, hot pressurizer technique, *etc.*<sup>29</sup> However, obtaining a bioplastic blend of PLA/PBS with good miscibility is challenging because of the different chemical properties of PLA and PBS. Herein, we have successfully prepared a bioplastic blend of PLA/PBS with an acceptable extent of miscibility using a simple solution casting method. The pristine films of PLA were obtained by stirring 4 weight% of PLA solution in chloroform at  $65^\circ \text{ C}$  for 4 h (Fig. 1 and Fig. S1). A similar process was applied for preparing the PLA/PBS blends by changing the percentages of PLA and PBS to 80/20, 50/50 and 20/80 and the resulting films are shown in Fig. 1. The thickness of the PLA and PLA/PBS blends is  $\sim 4.1 \pm 0.1 \mu\text{m}$  obtained using a profilometer (Fig. S2).

At the beginning, the miscibility of the PLA/PBS blends of 80/20, 50/50, and 20/80 was deciphered with the help of physicochemical analyses. First, FTIR spectroscopy was employed to understand the interaction between the functional groups in the PLA and PBS, as shown in Fig. 2. Briefly, the absorption at  $2922 \text{ cm}^{-1}$  is attributed to the stretching of the C–H bond of the main polymer chain of PLA and PBS. Next, the

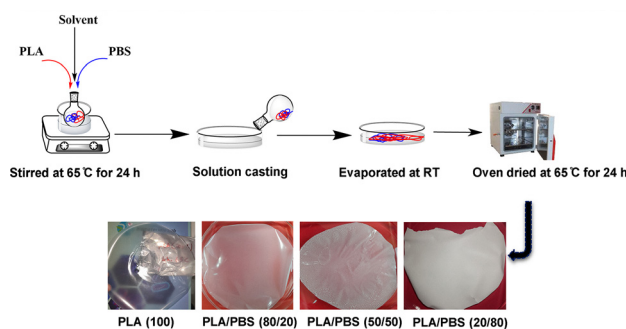


Fig. 1 Schematic representation to prepare pristine PLA films and PLA/PBS blended bioplastic films using the solution casting method (top row), and the second row shows the digital images of casted PLA (100%), PLA/PBS (80/20), PLA/PBS (20/80) and PLA/PBS (50/50), respectively.



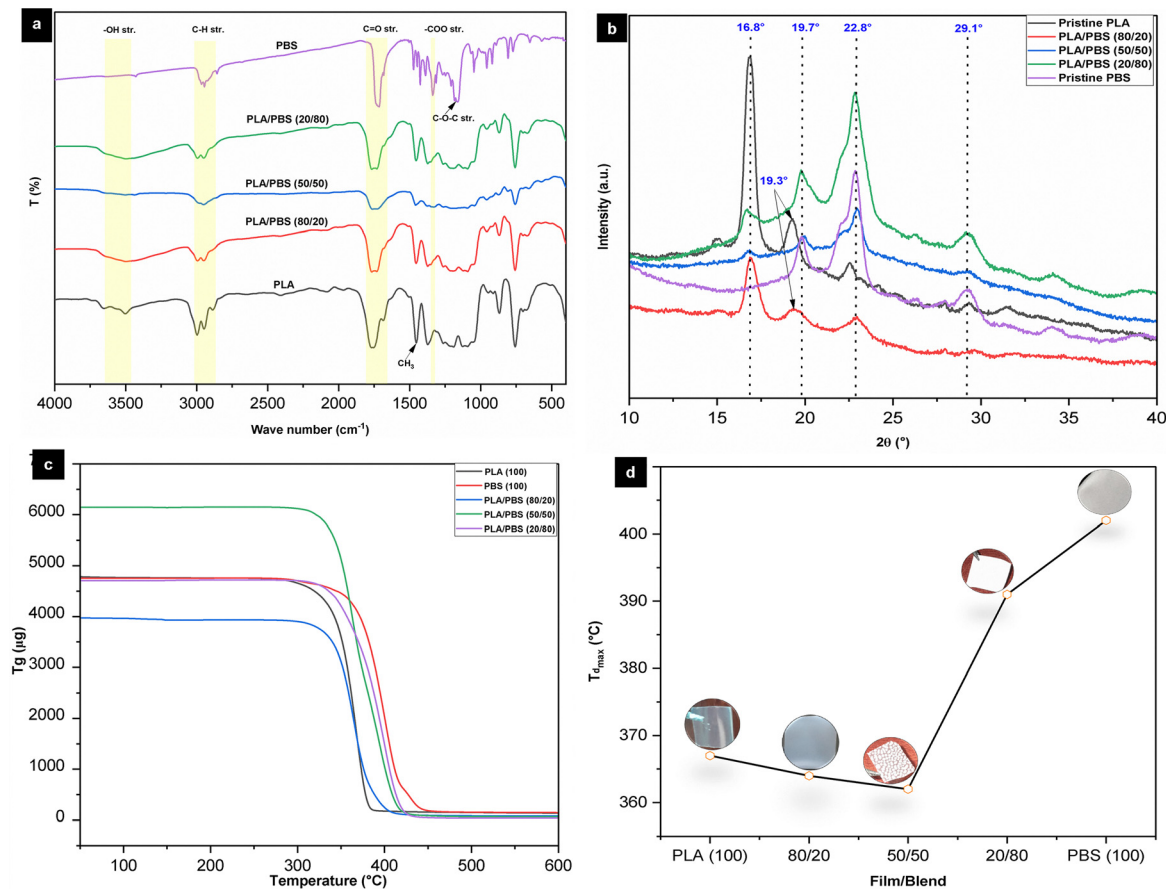


Fig. 2 The FTIR spectra (a), PXRD pattern (b), TGA curves (c) and  $T_{d,max}$  trends (d) of the prepared pristine PLA, pristine PBS films and PLA/PBS blended films, respectively.

intense vibrations at  $1715\text{ cm}^{-1}$  are related to the ester carbonyl ( $-\text{O}-\text{C}=\text{O}$ ) in the PLA and vibrations at  $1328\text{ cm}^{-1}$  correspond to the elongation vibration of the  $-\text{COO}$  bond of PLA. Furthermore,  $1160\text{ cm}^{-1}$  is a characteristic  $\text{C}-\text{O}-\text{C}$  stretching of the repeating unit ( $-\text{OCH}_2\text{CH}_2$ ) of PBS. As the PBS percentages increase, OH stretching was also increased gradually in PLA/PBS (20/80) due to the availability of free  $-\text{OH}$  groups in the blend, thereby confirming the interaction between the PLA and PBS chains in the blend.<sup>29,35,36</sup> Also,  $\text{C}-\text{O}-\text{C}$  stretching was only observed in pristine PBS and not found upon adding PLA to obtain PLA/PBS blends. In PLA/PBS (50/50), the  $\text{C}=\text{O}$  stretching frequency was observed with less intensity, unlike other blends, and replicated spectra were observed for PLA/PBS (80/20 and 20/80) (Fig. 2a).

Next, powder XRD (PXRD) was employed to understand the crystallinity of the plastic films (Fig. 2b). In particular,  $2\theta$  angles located at  $16.8^\circ$ ,  $19.3^\circ$ , and  $22.8^\circ$  are attributed to pristine PLA according to a previous report.<sup>12,33,37</sup> Furthermore, three peaks located at  $19.7^\circ$ ,  $21.7^\circ$ , and  $22.8^\circ$  are related to the pristine PBS with the (020), (021), and (110) planes, respectively, as reported earlier.<sup>29</sup> Upon obtaining the PLA/PBS blends, the resulting films of PLA/PBS (80/20) possess similar crystallinity to the pristine PLA due to a higher percentage of PLA compared to PBS. However, the PLA/PBS films (50/50 and 20/80) showed the characteristic peaks for both PLA and PBS because of the

successful formation of the blended plastic films, which were not present in the pristine PLA or PBS films. Hence, the PLA/PBS (50/50) and PLA/PBS (20/80) blends showed higher miscibility than the PLA/PBS (80/20) blend. Furthermore, thermogravimetric analysis (TGA/DTG, Fig. 2c and d) data show that both the pristine films and PLA/PBS blends show a single degradation curve, confirming successful blend formation between PLA and PBS.<sup>29</sup> This is not commonly observed for the blended plastic obtained using mechanical and other film-forming methods.<sup>12,33,38</sup> However, PLA/PBS (50/50) showed minor deviation as observed in the DTG plot (shown in Fig. S3, SI). Importantly, the PLA/PBS blends were found to have lower  $T_{d,max}$  temperature compared to the pristine PLA or PBS films, confirming that the PLA/PBS blends have less thermal stability than the pristine films of PLA and PBS, which may result in higher degradability of the blends over the pristine films.<sup>28,39</sup> Overall, the FTIR, PXRD and TGA results are in agreement with blend formation between PLA and PBS.

Next, DSC was also employed to further confirm the miscibility of PLA and PBS in the obtained blend plastic films by finding the glass transition temperature ( $T_g$ ), melting temperature ( $T_m$ ), and cold crystalline temperature ( $T_{cc}$ ) of the pristine polymers and blends (Fig. 3a). From the DSC plots, it is observed that the  $T_m$  of all the PLA/PBS blends is reduced compared to the pristine films (PLA or PBS), except PLA/PBS



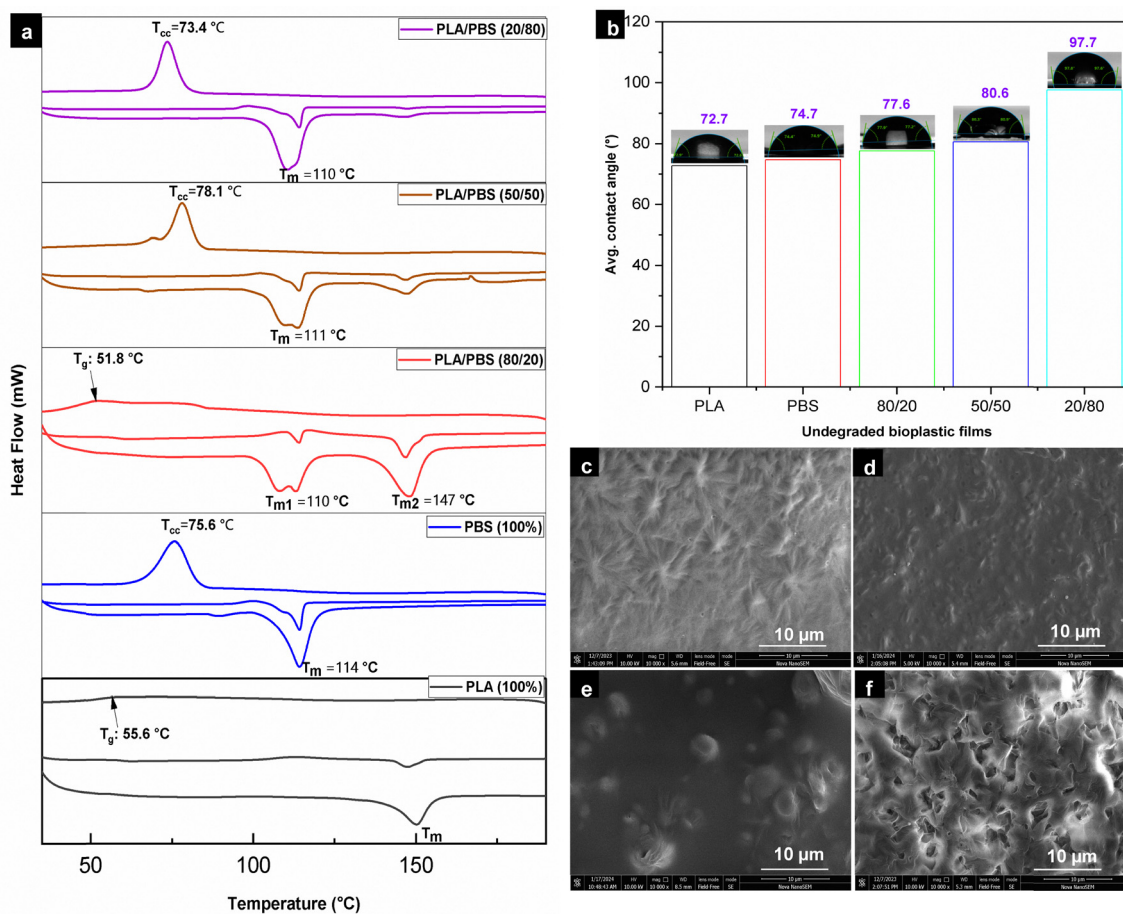


Fig. 3 DSC curves (a) and WCA measurements (b) of the pristine and blended films, respectively. SEM images of the pristine PLA and PLA/PBS blends of 80/20, 50/50, and 20/80 are shown in (c)–(f), respectively.

(80/20), since it shows two  $T_m$  at 110 °C and 147 °C, suggesting the immiscibility of PLA and PBS. However, the PLA/PBS (50/50) and PLA/PBS (20/80) blends show only one  $T_m$  at 110 °C, confirming the impressive phase miscibility between PLA and PBS at these two particular ratios, and also suggesting the uniform crystallinity in the blended films in comparison with reported works with other blending techniques.<sup>39,40</sup> Furthermore, water contact angle (WCA) measurements (Fig. 3b) reveal that the surface hydrophilicity decreased as the percentage of PBS was increased in the blends, which could be attributed to the presence of more ester groups in PBS that make the blend more hydrophobic.<sup>29,35,41</sup> Hence, PLA/PBS blends could be fascinating for packaging applications. Finally, SEM analysis was used to understand the morphology of the obtained blended films of PLA/PBS (Fig. 3c–f). First, pristine PLA films were found to have a smooth and shielded surface with spherulite-like morphology.<sup>37</sup> However, the PLA/PBS blend films show a rough morphology with cavities, and these features increase as the percentage of PBS increases in the blends, starting from 80/20 to 20/80 of PLA/PBS.<sup>33,41</sup> In addition, the blended films of PLA/PBS were found to have smoother and denser morphology than those obtained using other methods, including a melt compounding process.<sup>13,29,37</sup>

**2.6.2. RAB of the PLA and PLA/PBS blended films and powder.** We proposed to develop a test-tube model “rapid and accelerated biodegradation (RAB)” involving treating the bioplastic material (films or powder forms) with the respective microbial enzymes under accelerated conditions (Fig. 4 and Fig. S4).<sup>27</sup> RAB involves the degradation varying with multiple parameters (high temperature, varying the particle size, addition of enzyme additives, and optimising pH), which were tested to develop a simple test-tube model biodegradation test for the PLA/PBS bioplastic blends.<sup>42</sup> RAB was deployed to study the biodegradability of the PLA/PBS blends in the form of thin films and their powder form (particle size ranges 200–355  $\mu\text{m}$  and 500–700  $\mu\text{m}$ ) by treating with selected microbial enzymes. The extent of biodegradation under RAB conditions was followed by assessing the physicochemical properties (miscibility and compatibility, structural changes, morphology, and hydrophobicity) of the degraded plastic samples (films/powder). Techniques such as FTIR, PXRD, thermal analysis (TGA/DSC), contact angle (WCA) measurements, including electron microscopy (SEM) and optical microscopy (OM) were used to study the changes in the physicochemical properties of the blends.

*2.6.2.1. RAB study of PLA/PBS blended bioplastic films and powders using mobilized proteinase K.* RAB is one of the *in vitro*



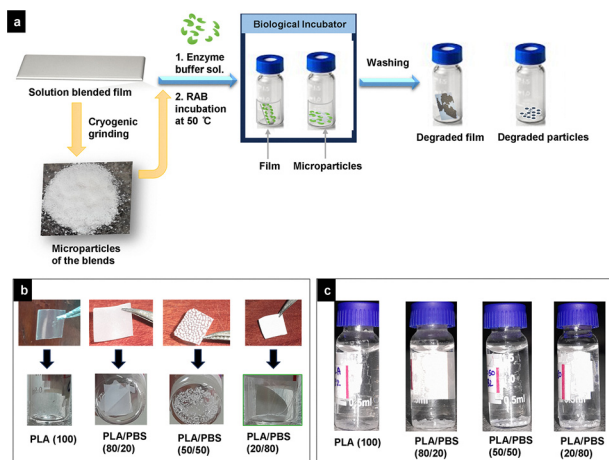


Fig. 4 Schematic representation of the RAB of PLA/PBS blended films and powder samples by treating with microbial enzymes (a). Pristine PLA and PLA/PBS blends (80/20, 50/50 and 20/80) before and after degradation under RAB conditions for films (b) and powder samples (c), respectively, treated with microbial enzymes under RAB.

controlled real-time degradation experiments with an accelerated condition to anticipate the maximum extent of degradation of synthetic biopolymers and their blends.<sup>28,35,43,44</sup> Weight loss analysis of the samples was carried out through the difference in mass before and after treatment to evaluate the degradation of the film samples under RAB conditions. It was found that the PLA/PBS (50/50) blend has the highest weight loss after 7 days of treatment compared to other blends and pristine PLA (Fig. 5a), which was also supported by observing

the complete breakage of the blend film into powder-like particles (Fig. 4b and Fig. S4a). The highest degradation of the PLA/PBS (50/50) blend film could be because of the uneven surface with a porous nature (SEM images, Fig. 3d). Therefore, the porous nature of the PLA/PBS (50/50) films is more likely to cause the highest degradation, thereby leading to weight loss. On the other side, 7 days of treatment with microbial enzyme caused the pristine PLA film and PLA/PBS (80/20 and 20/80) blends to be brittle and broken into large pieces (especially PLA/PBS-80/20, Fig. 4b and Fig. S4a). Next, weight loss measured after 12 h, 3 days and 7 days of treatment (Fig. 5a) for the pristine PLA film was very low, which could be attributed to the PLA film's smoothness and higher  $T_m$  compared to the PLA/PBS blends.<sup>45,46</sup> This is more evident for the PLA/PBS blend (50/50), having the lowest  $T_m$  as per DSC plots and rough surfaces (Fig. 3d).<sup>46</sup> In the case of powder samples (size 500–700  $\mu\text{m}$ , Fig. 5b) degradation under RAB conditions using proteinase K, the PLA/PBS-80/20 blend powder underwent the highest degradation compared to the other blends and PLA. This could be attributed to the higher surface area of the microparticles. Similar degradation of powder samples of PLA/PBS blend particles (size 200–355  $\mu\text{m}$ , Fig. 5c) was found to occur, where degradability was reduced as the percentage of PBS was decreased in the blend. Overall, the blend powder samples with 200–355  $\mu\text{m}$  particles were degraded slightly more than those with particles of 500–700  $\mu\text{m}$ . This could be due to the higher surface area available for 200–355  $\mu\text{m}$  particles over 500–700  $\mu\text{m}$  particles. Next, GPC was performed to estimate the molecular weight loss of the PLA plastic films and powders after treatment with proteinase K for 7 days, where the analysis

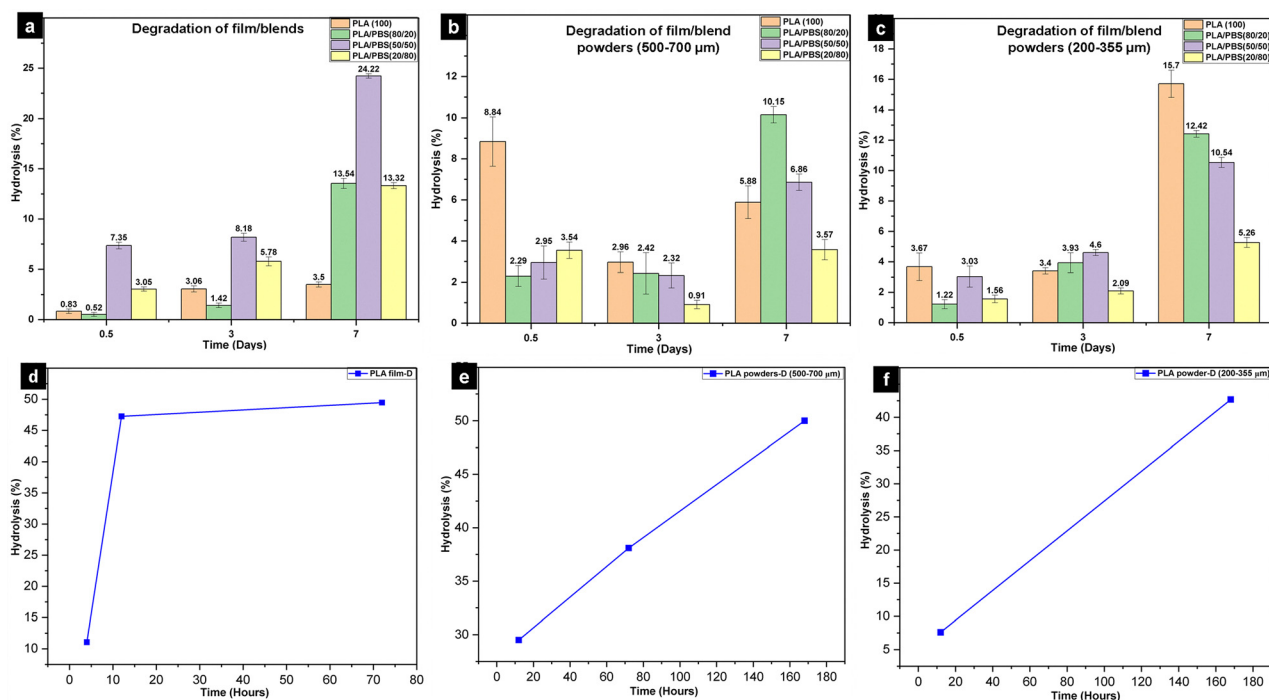


Fig. 5 Physical weight loss of (a) PLA/PBS blended films, (b) PLA/PBS blended powders, (500–700  $\mu\text{m}$ ) and (c) PLA/PBS blended powders (200–355  $\mu\text{m}$ ), and (d), (e) and (f) shows the molecular chain ( $M_n$ ) loss of pristine PLA in film and powders, respectively, that were obtained from GPC analysis.



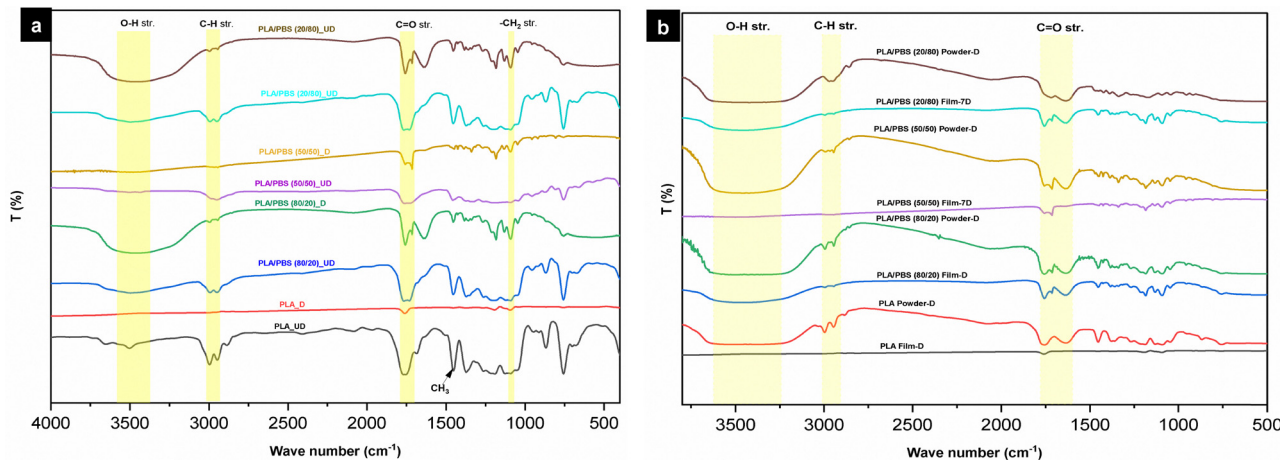


Fig. 6 FTIR spectra of (a) undegraded (UD), degraded (D) and pristine PLA films and PLA/PBS blended films; (b) a comparison between degraded PLA/PBS blended films and their powders under RAB conditions after 7 days by proteinase K.

was not possible for the blends, done only for the pristine PLA films and powder samples (Fig. 5d–f). The results confirmed that the total chain degradation or hydrolysis was  $\sim 47\%$  within the first 12 h of treatment, and reached nearly saturation (49%) by 72 h for PLA in the film (Fig. 5d and Table S3). Notably, chain loss or degradation for the PLA powder samples (for both 500–700  $\mu\text{m}$  particles and 200–355  $\mu\text{m}$  particles, Fig. 5e and f, and Table S4) was gradually increased until 7 days, unlike in the film samples, where the chain loss was saturated after 3 days. Also, GPC confirmed that the 500–700  $\mu\text{m}$  range PLA powder samples were degraded to 46% and the 200–355  $\mu\text{m}$  range PLA powder degraded to 43% by 7 days. Here, the larger particles (500–700  $\mu\text{m}$ ) were degraded slightly more than the smaller range particles (200–355  $\mu\text{m}$ ). This is possibly due to variation in the shape and crystallinity of the micro-particles, which might have been induced by cryogenic grinding or due to the uneven enzyme distribution in the specific

experiments. The mechanism of enzymatic degradation is shown in Scheme S1.

Next, FTIR analysis was performed to understand the structural changes or functional groups of the PLA/PBS blends after treating with proteinase K (Fig. 6) for 7 days. First, a drastic reduction in the C–H stretching and ester–O–C=O stretching frequencies was observed for the degraded pristine PLA film (named PLA-D, Fig. 6a), which confirms the cleavage of the ester linkage in the polymeric chain.<sup>42,45</sup> Next, FTIR analysis for the degraded PLA/PBS blends (labelled as PLA/PBS-D) shows the presence of broad vibrations at  $\sim 3300$  to  $3500\text{ cm}^{-1}$ , which might correspond to the presence of free –OH groups, which were formed after the enzymatic hydrolysis of PLA alone (Fig. S4, S1). However, these broad bands were absent in the undegraded PLA/PBS (untreated at 0 h sample). Similarly, in the case of degraded PLA/PBS (20/80), broadening of –OH and shifting of the C=O frequencies support that the PLA/PBS blends underwent enzymatic

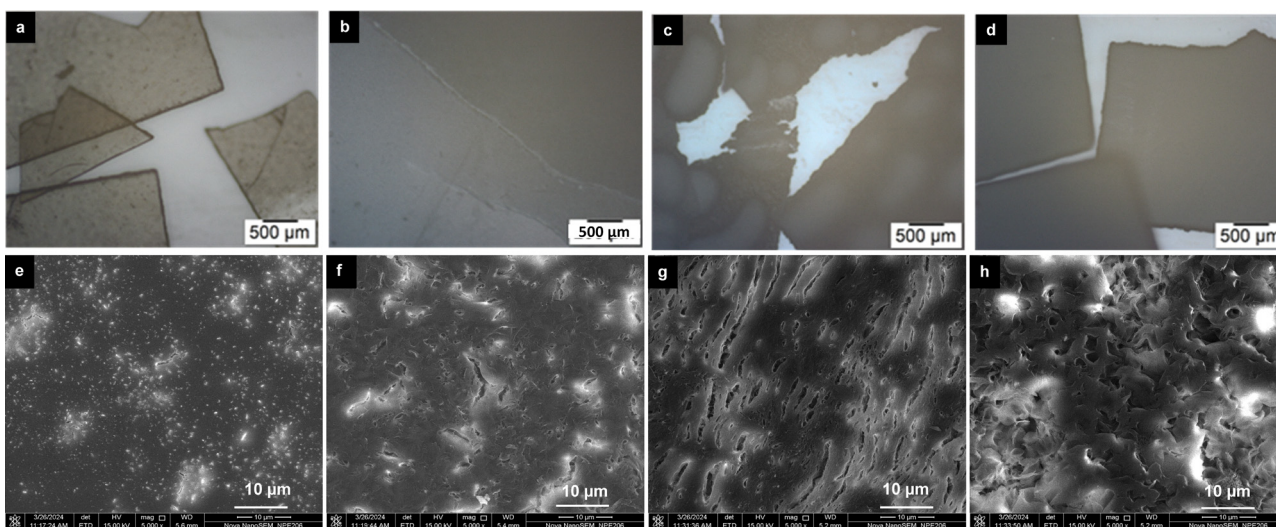
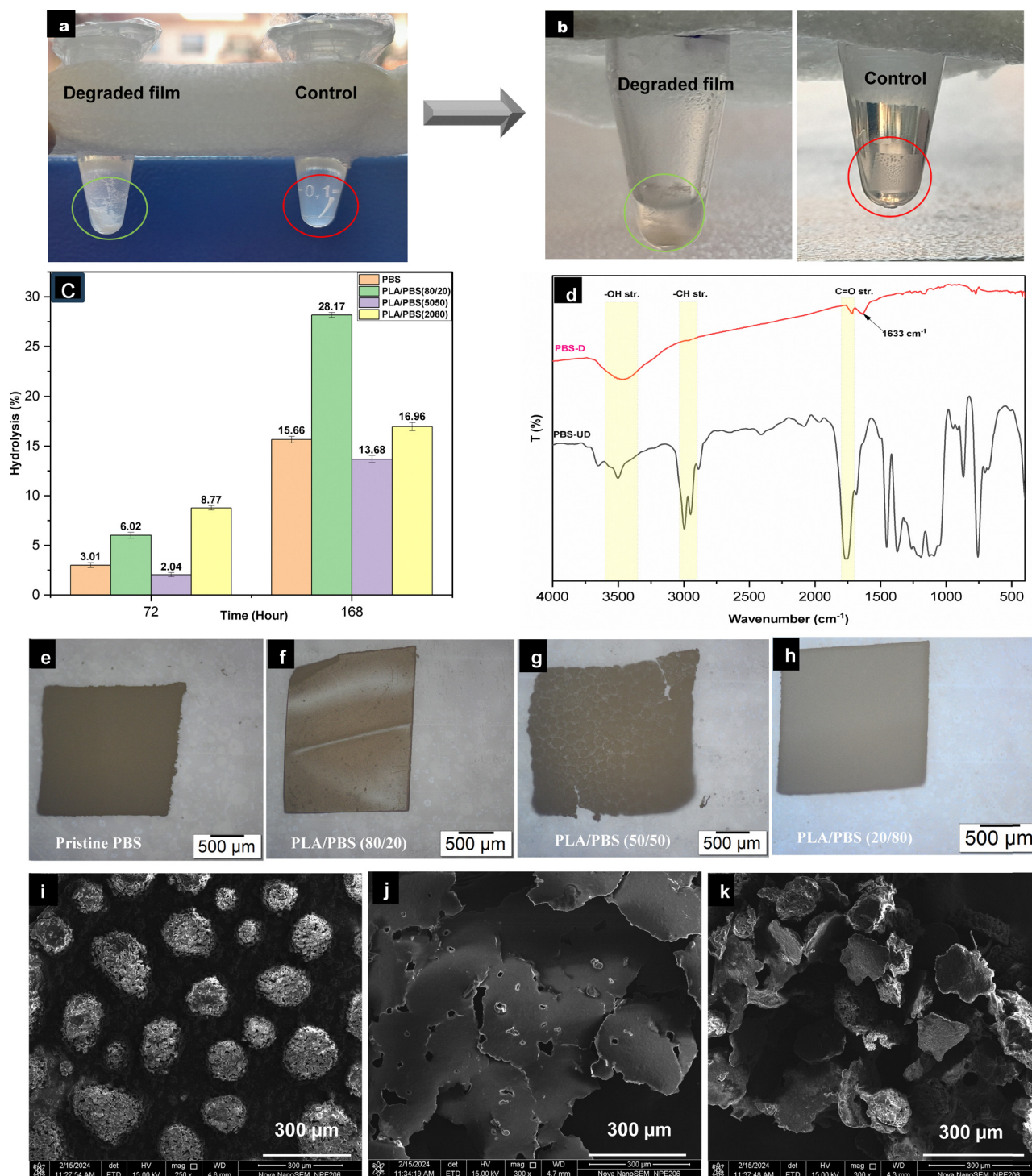


Fig. 7 OM images of degraded (a) PLA film and PLA/PBS blends (b) 80/20, (c) 50/50, and (d) 20/80 on the 3rd day and SEM images of degraded (e) PLA films and PLA/PBS blends (f) 80/20, (g) 50/50, and (h) 20/80 after 7 days under RAB by proteinase K.



hydrolysis.<sup>29,33,44,46</sup> Similar changes were observed for the powder samples of PLA and the PLA/PBS blends after treating with protease K for 7 days (Fig. 6b and Fig. S5a), confirming the enzymatic hydrolysis of PLA in the PLA/PBS blend powder samples.

To support this, PXRD was also employed, where the PXRD results show no change in the crystallinity of the PLA film and PLA powder samples before and after degradation for 7 days (Fig. S5b).<sup>33</sup> However, there was a change in the crystallinity



**Fig. 8** (a) and (b) Digital photos of the vials containing degraded PLA/PBS (50/50) blend on the 3rd day and 7th day, respectively; (c) the relative degradation plot of all three PLA/PBS blends after treatment with lipase enzyme; (d) the FTIR spectra of pristine PBS before and after degradation by lipase; (e)–(h) the optical microscopy images of the degraded pristine PBS film and three PLA/PBS blended films after 7 days, respectively; and (i)–(k) the SEM images of the degraded PLA/PBS (50/50) blend at the 12th h, 3 days, and 7 days, respectively.



only for PLA/PBS (50/50) blend samples after enzymatic treatment for 7 days (Fig. S5b–f). However, PLA/PBS (50/50) shows some splitting or shoulder peak at 19.8°, which might be due to the structural changes in the blend after 7 days (Fig. S5e). The crystallinity changes observed mainly for the PLA/PBS (50/50) blend could be attributed to its lowest melting temperature ( $T_m$ , Fig. 3a) and having a highly rough surface morphology compared to the other blends (Fig. 3d–f).<sup>34</sup> Furthermore, SEM and OM images also supported the degradation of the film samples of the PLA and PLS/PBS blends after up to 7 days of enzymatic treatment (Fig. 7 and Fig. S6, S7). Optical images demonstrate that broken films were observed in the PLA and PLS/PBS blend film samples, suggesting that degradation had occurred (Fig. 7a–d).

In addition, more porous and damaged areas in the films of PLA and the PLA/PBS blends were observed in the SEM images (Fig. 7e–h). However, such significant morphological changes were not observed for the powder samples of PLA and the PLA/PBS blends, which could be due to the uneven surface morphology with an irregular shape, making it challenging to identify the reduction of size and morphology of the powder particles (Fig. S8). Furthermore, water contact angle (WCA) measurements were performed, and the results confirmed that the blended films were flat and flexible in the beginning, *i.e.* before biodegradation (Fig. 4b). However, the PLA films and PLA/PBS blend films became brittle and curvy (except PLA/PBS-50/50) after enzymatic treatment, and therefore we could not measure the WCA of the blends (Fig. S9a–e). The WCA of the PLA/PBS (50/50) film was reduced to 31% after 12 h of degradation (Fig. S9c), resulting in an increase in hydrophilicity by 12 h of degradation, which further supports the degradation of PLA/PBS (50/50) occurring to a greater extent than the other blended films.<sup>35</sup> Therefore, such a PLA/PBS (50/50) blend could be interesting with higher biodegradability over the other blends.

**2.6.2.2. Degradation of pristine PLA using lipase immobilised in acrylic resin in an organic solvent.** Next, the impact of organic solvents on the enzymatic degradation of PLA was studied using toluene as the solvent under RAB conditions.<sup>22,47</sup> The results confirmed that the prepared PLA film did not dissolve completely throughout incubation, and the resulting film was recovered for GPC analysis. The molecular weight loss after 72 h was found to be only 12.45%, which is nearly 4 times less than that in the proteinase K-mobilised enzyme treated under RAB conditions (Table S6). The plausible reason could be that immobilised enzymes might be unable to bind to the PLA films or have low solubility in toluene, resulting in a lower percentage of degradation.<sup>48</sup> As the PLA film alone degraded poorly in the organic solvent, the PLA/PBS blends were not studied under such conditions.

**2.6.2.3. Degradation of pristine PBS and PLA/PBS blends using lipase.** As proteinase K targets the PLA chain in the PLA/PBS blend plastic, lipase from *Pseudomonas* sp. can degrade the PBS chain in the PLA/PBS blends.<sup>30–32</sup> Hence, we attempted to

understand the degradation of PBS in pristine PBS films and PLA/PBS blend films by treating them with lipase under RAB conditions (Fig. 4). PBS or PLA/PBS blend films were incubated in 0.1 M phosphate buffer at pH 7.2 (Fig. 8a and b).<sup>29</sup> It was found that PLA/PBS (80/20) films degraded to a larger extent than pristine PBS and PLA/PBS films (50/50 and 20/80, Fig. 8c) after 7 days. However, pristine PBS, PLA/PBS (50/50) and PLA/PBS (20/80) showed similar degradation after 7 days. PLA/PBS (80/20) degraded up to ~28% on the 7th day of study, which may be attributed to the  $T_m$  data of the blend. PLA/PBS (20/80) degraded to a higher extent on the 3<sup>rd</sup> day of study, as it has a higher percentage of PBS in it.

Next, FTIR spectra of the PBS and PLA/PBS blends were analysed to understand their enzymatic hydrolysis. First, the degraded PBS film showed a broadened –OH stretching frequency and shifting of the C=O frequency from ~1725–1715  $\text{cm}^{-1}$  to ~1620–1633  $\text{cm}^{-1}$  (Fig. 8d), which could be due to the hydrolysis of the ester group to generate free COOH groups and the C–H stretching frequency also vanished after degradation.<sup>29</sup>

Additionally, optical images of the degraded samples revealed that the morphology of the films was not changed much except for the PLA/PBS (50/50) blend after treatment for 7 days (Fig. 8e–h), where the PLA/PBS (50/50) film was found to be broken with a porous nature after the degradation. In support of this, SEM analysis of the PLA/PBS (50/50) blend suggested that the film was broken down into smaller films and had several pores (Fig. 8i and j). Subsequently, it turned entirely to microparticles after 1 minute of sonication (Fig. 8k). The highest degradation found in the PLA/PBS (50/50) blend film compared to other blends could be attributed to the film's rough morphology, arrangement of the two polymers in the matrix, and crystallinity of the mixed blend ( $T_m$  plot) compared to other films.<sup>34,43</sup>

### 3. Conclusion

First, we developed a simple solution casting method for preparing a PLA/PBS blended biodegradable bioplastic with high miscibility (especially for a 50/50 and 20/80 ratio) based on thermal gravimetric (DSC and TGA) and electron microscopy analyses. Other physicochemical characterisation using FTIR, PXRD, including water contact angle measurements, and optical microscopy results also confirmed the successful preparation of the blended bioplastic of PLA/PBS. We believe that the developed solution casting method could be applied to make miscible bioplastic blends of PLA/PBS, which have many biomedical and packaging applications. Second, we developed an efficient test-tube method to assess the biodegradability of the obtained PLA/PBS bioplastic blends in the form of films and powders by treating with appropriate microbial enzymes (proteinase K and lipase) under rapid accelerated biodegradation (RAB) conditions (pH, high temperature incubation, microparticles and organic solvent). Overall, the PLA/PBS (50/50) blended bioplastic films degraded to a greater extent, 24.2%



within 7 days with proteinase K in aqueous medium, compared to the other PLA/PBS blends. Furthermore, the powder forms of the pristine PLA and PLA/PBS blended bioplastic underwent RAB by proteinase K, and it was found that surface area plays a vital role in enhancing the biodegradation. In addition, the pristine PLA film could not be degraded significantly using immobilised (acrylic resin) lipase in a non-aqueous medium, which deciphered the advantages of aqueous medium for better biodegradability of bioplastic blends. Finally, we examined the biodegradation of PBS and PLA/PBS blends by lipase (*Pseudomonas* sp.) under RAB conditions. The results confirm that PLA/PBS (80/20) degraded faster than the PLA/PBS (20/80) and PLA/PBS (50/50) blends and pristine PBS. Overall, our test-tube model RAB studies demonstrated that the PLA/PBS blend bioplastic films showed faster degradation (within 7 days) compared to the blends obtained from other techniques (melt blending, mechanical extrusion, *etc.*). The test-tube model RAB degradation could be applied for understanding the rapid accelerated biodegradation of other bioplastic blends by simply treating them with appropriate microbial enzymes under accelerated conditions (pH, temperature, size of the plastic, solvent, *etc.*). Our RAB model could be a simple test-tube model to predict the biodegradability of the blended bioplastic by incubating with the selected microbial enzyme (*e.g.*, isolated from microbes present in the soil). Also, the RAB model could be used to screen and compare newly developed blended or biodegradable bioplastics in a shorter time than the standardised biodegradation tests. However, correlating the accelerated or rapid biodegradation of bioplastic with real-time or practical degradation is difficult. Since practical or environmental degradation conditions will be very different from the accelerated or RAB model, the biodegradation of the bioplastic will be studied.

## Author contributions

Shreetam Parida: experimental, methodology, characterisations, data analyses and original draft; Nivethitha Ashok: experimental and formal analysis; Dr Rajendra Kurapati: project conceptualisation, methodology, supervision and draft revision.

## Conflicts of interest

There are no conflicts to declare.

## Data availability

The data supporting this article have been included as part of the supplementary information (SI). Supplementary information is available. See DOI: <https://doi.org/10.1039/d5ma00690b>.

Any additional data required for replication or further inquiry can be obtained upon request.

## Acknowledgements

The authors are thankful to the Department of Biotechnology (DBT), Govt of India, for supporting and funding the project with reference number “BT/PR48101/BCE/8/1808/2023”. The authors acknowledge IISER Thiruvananthapuram, Kerala, India, for providing the necessary laboratory and characterisation facilities. They are also thankful to Dr Bhoje Gowd E., CSIR-NIIST, Thiruvananthapuram, Polymer Science division, for water contact angle measurements and necessary suggestions.

## Notes and references

- 1 K. J. Groh, T. Backhaus, B. Carney-Almroth, B. Geueke, P. A. Inostroza, A. Lennquist, H. A. Leslie, M. Maffini, D. Slunge, L. Trasande, A. M. Warhurst and J. Muncke, *Sci. Total Environ.*, 2019, **651**, 3253–3268.
- 2 W.-H. Hsu, Y.-Z. Chen, Y.-T. Chiang, Y.-T. Chang, Y.-W. Wang, K.-T. Hsu, Y.-Y. Hsu, P.-T. Wu and B.-H. Lee, *Nat. Commun.*, 2025, **16**, 5026.
- 3 P. Shreetam, A. Nivethitha and K. Rajendra, *Ann. Biomed. Sci. Eng.*, 2024, **8**, 004–010.
- 4 M. Mangal, C. V. Rao and T. Banerjee, *Polym. Int.*, 2023, **72**, 984–996.
- 5 M. Nofar, D. Sacligil, P. J. Carreau, M. R. Kamal and M. C. Heuzey, *Int. J. Biol. Macromol.*, 2019, **125**, 307–360.
- 6 N.-A. Taib, M. Rahman, D. Huda, K. Kuok, S. Hamdan, M. K. Bakri, M. Julaihi and A. Khan, *Polym. Bull.*, 2022, **1**, 1–35.
- 7 BIOPLASTICS MARKET UPDATE 2021 | European Bioplastics, 2021, [https://docs.european-bioplastics.org/publications/market\\_data/Report\\_Bioplastics\\_Market\\_Data\\_2021\\_short\\_version.pdf](https://docs.european-bioplastics.org/publications/market_data/Report_Bioplastics_Market_Data_2021_short_version.pdf).
- 8 Z. H. W. Easton, M. A. J. Essink, L. Rodriguez Comas, F. R. Wurm and H. Gojzewski, *Macromol. Chem. Phys.*, 2023, **224**, 2200421.
- 9 H. Cai, C. Cao, Y. Zheng, D. Liu, X. Xia, X. Sun, X. Liu, L. Xiao, Q. Qian and Q. Chen, *Macromol. Mater. Eng.*, 2023, **308**, 2200581.
- 10 E. C. Van Roijen and S. A. Miller, *Resour., Conserv. Recycl.*, 2022, **181**, 106236.
- 11 N. C. Giri, V. Verma and B. P. Patro, in *Assessing the Effects of Emerging Plastics on the Environment and Public Health*, ed. S. H. Joo, IGI Global, Hershey, PA, USA, 2022, pp. 249–283, DOI: [10.4018/978-1-7998-9723-1.ch011](https://doi.org/10.4018/978-1-7998-9723-1.ch011).
- 12 R. Wang, S. Wang, Y. Zhang, C. Wan and P. Ma, *Polym. Eng. Sci.*, 2009, **49**, 26–33.
- 13 T. Zhao, J. Yu, X. Zhang, W. Han, S. Zhang, H. Pan, Q. Zhang, X. Yu, J. Bian and H. Zhang, *Polym. Bull.*, 2023, **81**, 1–24.
- 14 W. Pivsa-Art, S. Pivsa-Art, K. Fujii, K. Nomura, K. Ishimoto, Y. Aso, H. Yamane and H. Ohara, *J. Appl. Polym. Sci.*, 2015, **132**, 41856.
- 15 K. Shi, Z. Bai, T. Su and Z. Wang, *Int. J. Biol. Macromol.*, 2019, **126**, 436–442.



- 16 L. Filiciotto and G. Rothenberg, *ChemSusChem*, 2021, **14**, 56–72.
- 17 A. Folino, D. Pangallo and P. S. Calabrò, *J. Environ. Chem. Eng.*, 2023, **11**, 109424.
- 18 J.-G. Rosenboom, R. Langer and G. Traverso, *Nat. Rev. Mater.*, 2022, **7**, 117–137.
- 19 S. Andréia da Silva, D. J. L. Faccin and N. S. M. Cardozo, *ACS Sustainable Chem. Eng.*, 2024, **12**, 11856–11865.
- 20 J. Šerá, L. Serbruyns, B. De Wilde and M. Koutný, *Polym. Degrad. Stab.*, 2020, **171**, 109031.
- 21 S. Chinaglia, M. Tosin and F. Degli-Innocenti, *Polym. Degrad. Stab.*, 2018, **147**, 237–244.
- 22 M. H. Aris, M. S. M. Annuar and T. C. Ling, *Polym. Degrad. Stab.*, 2016, **133**, 182–191.
- 23 A. N. Mistry, B. Kachenchart, A. Wongthanaroj, A. Somwangthanaroj and E. Luepromchai, *Polym. Degrad. Stab.*, 2022, **202**, 110051.
- 24 Z. Montazer, M. B. Habibi Najafi and D. B. Levin, *Can. J. Microbiol.*, 2019, **65**, 224–234.
- 25 J. Kaushal, M. Khatri and S. K. Arya, *Cleaner Eng. Technol.*, 2021, **2**, 100083.
- 26 H. Jeong, J. Rho, J.-Y. Shin, D. Y. Lee, T. Hwang and K. J. Kim, *Biomed. Eng. Lett.*, 2018, **8**, 267–272.
- 27 S. Grima, V. Bellon-Maurel, P. Feuilloley and F. J. Silvestre, *J. Polym. Environ.*, 2000, **8**, 183–195.
- 28 Y. Kikkawa, H. Abe, T. Iwata, Y. Inoue and Y. Doi, *Bio-macromolecules*, 2002, **3**, 350–356.
- 29 X. Hu, T. Su, P. Li and Z. Wang, *Polym. Bull.*, 2018, **75**, 533–546.
- 30 K. Mukai, Y. Doi, Y. Sema and K. Tomita, *Biotechnol. Lett.*, 1993, **15**, 601–604.
- 31 Y. Tokiwa and T. Suzuki, *Nature*, 1977, **270**, 76–78.
- 32 C. W. Lee, Y. Kimura and J.-D. J. M. R. Chung, *Macromol. Res.*, 2008, **16**, 651–658.
- 33 F.-L. Chang, B. Hu, W.-T. Huang, L. Chen, X.-C. Yin, X.-W. Cao and G.-J. He, *Polymer*, 2022, **259**, 125336.
- 34 H. Cai, V. Davé, R. A. Gross and S. P. McCarthy, *J. Polym. Sci., Part B: Polym. Phys.*, 1996, **34**, 2701–2708.
- 35 S. Li and S. McCarthy, *Macromolecules*, 1999, **32**, 4454–4456.
- 36 A. Gowman, T. Wang, A. Rodriguez-Urbe, A. K. Mohanty and M. Misra, *ACS Omega*, 2018, **3**, 15205–15216.
- 37 J. W. Park and S. S. Im, *J. Appl. Polym. Sci.*, 2002, **86**, 647–655.
- 38 E. Hassan, Y. Wei, H. Jiao and Y. Muhuo, *J. Fibre Bioeng. Inf.*, 2013, **6**, 85–94.
- 39 B. Ahn, S. Kim, Y. Kim and J. Yang, *J. Appl. Polym. Sci.*, 2001, **82**, 2808–2826.
- 40 T. Qiu, M. Song, L. Zhao and M. Processes, *Mech. Adv. Mater.*, 2016, **2**, 7.
- 41 W. Yu, L. Sun, M. Li, M. Li, W. Lei and C. Wei, *Polymers*, 2023, **15**, 4305.
- 42 R.-S. Rose, K. H. Richardson, E. J. Latvanen, C. A. Hanson, M. Resmini and I. A. Sanders, *Int. J. Mol. Sci.*, 2020, **21**, 1176.
- 43 Y. Tokiwa and B. P. Calabria, *Biotechnol. Lett.*, 2004, **26**, 1181–1189.
- 44 A. Rosato, A. Romano, G. Totaro, A. Celli, F. Fava, G. Zanaroli and L. J. P. Sisti, *Polymers*, 2022, **14**, 1850.
- 45 H. Fukuzaki, M. Yoshida, M. Asano and M. Kumakura, *Eur. Polym. J.*, 1989, **25**, 1019–1026.
- 46 M. S. Reeve, S. P. McCarthy, M. J. Downey and R. A. J. M. Gross, *Macromolecules*, 1994, **27**, 825–831.
- 47 C. DelRe, Y. Jiang, P. Kang, J. Kwon, A. Hall, I. Jayapurna, Z. Ruan, L. Ma, K. Zolkin, T. Li, C. D. Scown, R. O. Ritchie, T. P. Russell and T. Xu, *Nature*, 2021, **592**, 558–563.
- 48 D. Edith and J.-L. Six, *J. Appl. Surf. Sci.*, 2006, **253**, 2758–2764.

